J. Fluid Mech. (1973), *vol.* 58, *part* 3, *pp.* 581–593
Printed in Great Britain

High-order moments of Reynolds shear stress fluctuations in a turbulent boundary layer

by R. A. ANTONIA AND J. D. ATKINSON
Department of Mechanical Engineering, University of Sydney

(Received 1 June 1972 and in revised form 24 October 1972)

The cumulant-discard approach is used to predict the third- and fourth-order moments and the probability density of turbulent Reynolds shear stress fluctuations uv, the streamwise and normal velocity fluctuations being represented by u and v respectively. Measurements of these quantities in a turbulent boundary layer are presented, with the required statistics of uv obtained by the use of a high-speed digital data-acquisition system. Including correlations between u and v up to the fourth order, the cumulant-discard predictions are in close agreement with the measurements in the inner region of the layer but only qualitatively follow the experimental results in the outer intermittent region. In this latter region, predictions for the third- and fourth-order moments of uv are also obtained by assuming that the properties of both turbulent and irrotational fluctuations are Gaussian and by using some of the available conditional averages of u, v and uv.

1. Introduction

Recent investigations by Frenkiel & Klebanoff (1967), Van Atta & Chen (1968) and Van Atta & Yeh (1970) have attempted both to measure and predict some of the higher order moments of the streamwise velocity fluctuations in the turbulent flow downstream of a grid. Frenkiel & Klebanoff and Van Atta & Chen have shown that, although some of the higher even-order correlations at two points separated in time are quite closely predicted by assuming a Gaussian joint probability density, the successful prediction of the odd-order correlations requires the use of a non-Gaussian Gram–Charlier probability density. Van Atta & Yeh (1970) have found that, while the measured even-order correlations at four points separated in time may be quite closely predicted by the joint-Gaussian hypothesis, the generalized Gram–Charlier densities are required to describe the odd-order three-point correlations.

The present work is concerned with predicting some of the measured third- and fourth-order correlations of the important Reynolds shear stress fluctuations uv in a turbulent boundary layer. In a previous report (Antonia & Luxton 1971*b*), some of the characteristics of the streamwise fluctuations u, the normal fluctuations v and of the product uv in a turbulent boundary layer were examined in the light of current boundary-layer knowledge. In a first attempt to predict some of the higher order moments of uv it was assumed that the joint probability density of u and v was Gaussian, but this led to generally unsatisfactory predictions for the skewness and flatness factors of uv. Here, the cumulant-discard approach outlined in § 2 is used as a convenient way to include the non-Gaussian behaviour of u and v. The resulting predictions are compared with the measured skewness and flatness factors of uv in both smooth- and rough-wall boundary layers. The rough-wall results are included because, for the particular roughness geometry used, the characteristics of uv in the vicinity of the surface are markedly different from those observed near the smooth wall. The probability density derived by doing an inverse Fourier transform on the characteristic function used to define the cumulants is the same as the Gram–Charlier representation assumed by Frenkiel & Klebanoff and others. This probability density is compared with the experimental distributions in § 4.

Predictions for the third- and fourth-order moments of uv in the intermittent region of the layer are derived in § 5 by assuming that the intermittency characteristics of the flow are known. Because of the limited data available on conditional averages of u, v and uv it is assumed that both turbulent and irrotational fluctuations are independent Gaussian stationary random variables.

2. Skewness and flatness of uv by cumulant discard

If u and v are two random variables, their statistical properties are specified by their joint probability density $p_{uv}(u,v)$ or alternatively (see, for example, Lin 1967, pp. 26–30) by their joint characteristic function M_{uv}, which is the double Fourier transform of $p_{uv}(u,v)$:

$$M_{uv}(\xi,\eta) = \iint e^{i(u\xi+v\eta)} p_{uv}(u,v)\,du\,dv = \sum_{n=0}^{\infty} \frac{i^n}{n!} \overline{(u\xi+v\eta)^n}. \tag{1}$$

The coefficient of $\xi^j\eta^k$ in the above series expansion is $(i^{j+k}/j!\,k!)\,m_{jk}$, where m_{jk} represents the moment $\overline{u^jv^k}$. It is more convenient to use, instead of the moments m_{jk}, the cumulants or semi-invariants k_{jk} defined by

$$k_{jk} = \frac{1}{i^{j+k}} \frac{\partial^{j+k}}{\partial\xi^j\,\partial\eta^k} \ln M_{uv}(\xi,\eta)\big|_{\xi=\eta=0}. \tag{2}$$

If the exponential of both sides of (2) is taken and the resulting coefficients of $\xi^j\eta^k$ compared with those in (1) some of the main relations between the m_{jk} and k_{jk} (for $j,k \leqslant 4$) become, when u and v have zero mean and are normalized by dividing by their respective standard deviations,

$$\left.\begin{aligned}
&m_{11} = \overline{w} = r, \quad m_{30} = k_{30}, \quad m_{21} = k_{21}, \quad m_{40} = k_{40}+3, \quad m_{31} = k_{31}+3r,\\
&m_{22} = \overline{w^2} = k_{22}+2r^2+1,\\
&m_{33} = \overline{w^3} = k_{33}+k_{30}k_{03}+9k_{21}k_{12}+3k_{13}+9rk_{22}+3k_{31}+9r+6r^3,\\
&m_{44} = \overline{w^4} = k_{44}+k_{40}k_{04}+16k_{31}k_{13}+18k_{22}^2+4(k_{30}k_{14}+k_{03}k_{41})\\
&\quad +24(k_{21}k_{23}+k_{12}k_{32})+6(k_{24}+k_{42})+16rk_{33}+24(k_{21}k_{03}+k_{12}k_{30})\\
&\quad +36(k_{12}^2+k_{21}^2)+16rk_{30}k_{03}+144rk_{12}k_{21}+3(k_{04}+k_{40})+48r(k_{13}+k_{31})\\
&\quad +36(1+2r^2)\,k_{22}+9+72r^2+24r^4,
\end{aligned}\right\} \tag{3}$$

where w stands for the product uv and r is the usual correlation coefficient. One reason for the usefulness of the cumulants can be seen by studying the case where u and v are Gaussian, so that their joint density has the form

$$p_{uv}(u,v) \propto \exp\left[-(a_{11}u^2 + a_{12}uv + a_{22}v^2 + a_1 u + a_2 v)\right],$$

i.e. the exponential of a second-order polynomial in u and v. Then its Fourier transform $M_{uv}(\xi, \eta)$ will also have this form, so that $\ln M_{uv}$ will be a second-order polynomial in ξ and η. This means that all the k_{ij} except k_{10}, k_{01}, k_{20}, k_{11} and k_{02} will be zero. If, on the other hand, u and v are not Gaussian, the magnitude of these k_{ij} can be used as a measure of the non-Gaussianity. In particular, in the normalized case where $k_{20} = 1$, k_{30} is the skewness of u and k_{40} is its coefficient of excess (the flatness factor is $k_{40} + 3$). Since moments of u and v of order higher than four are seldom measured, the statistics of u and v are not completely determined. In order to proceed further some assumption concerning the unspecified k_{ij} is necessary. Provided that the departures of u and v from Gaussianity are not too large, a reasonable assumption appears to be that all k_{ij} for i and j greater than 4 are zero. Using relations (3), it is easy to show that the standard deviation σ, skewness S and flatness factor F of the centred variable $w - \overline{w}$ are given by

$$\sigma = \left[\overline{(w-\overline{w})^2}\right]^{\frac{1}{2}} = (1 + k_{22} + r^2)^{\frac{1}{2}}, \tag{4}$$

$$S = \frac{\overline{(w-\overline{w})^3}}{\sigma_w^3} = \frac{k_{30}k_{03} + 9k_{21}k_{12} + 3(k_{13} + k_{31}) + 6rk_{22} + 2r^3 + 6r}{(1 + k_{22} + r^2)^{\frac{3}{2}}} \tag{5}$$

and

$$\begin{aligned} F = \frac{\overline{(w-\overline{w})^4}}{\sigma_w^4} &= [k_{40}k_{04} + 16k_{31}k_{13} + 18k_{22}^2 + 24(k_{21}k_{03} + k_{12}k_{30}) \\ &+ 36(k_{12}^2 + k_{21}^2) + 12rk_{30}k_{03} + 108rk_{21}k_{12} + 3(k_{04} + k_{40}) + 36r(k_{13} + k_{31}) \\ &+ k_{22}(42r^2 + 36) + 9r^4 + 42r^2 + 9]/(1 + k_{22} + r^2)^2. \end{aligned} \tag{6}$$

In the special case where only the skewnesses and flatness factors of u and v and the correlation coefficient r are retained, (5) and (6) reduce to

$$S = [k_{30}k_{03} + 2r^3 + 6r]/(1 + r^2)^{\frac{3}{2}} \tag{5a}$$

and

$$F = \frac{k_{40}k_{04} + 12rk_{30}k_{03} + 3(k_{04} + k_{40}) + 9 + 42r^2 + 9r^4}{(1 + r^2)^2}. \tag{6a}$$

It is worth noting that the skewness S is independent of k_{40} and k_{04} while, for small values of r, the flatness factor F is only weakly dependent on k_{30} and k_{03}, the skewnesses of u and v respectively.

3. Comparison with experimental results

Measurements were made in both a smooth-wall and a rough-wall boundary layer at a free-stream velocity of approximately 5·5 m/s. The boundary layers developed in a zero pressure gradient and were approximately self-preserving at the station of measurement. The roughness surface consisted of strips of

0·318 cm square cross-section spanning the full width of the working section floor and placed at a streamwise pitch of 1·27 cm. At the measuring station, the boundary layer had a 99·5 % thickness of 5·0 cm over the smooth surface and of 7·1 cm for the rough surface condition.

The signals from an X-wire operated by two channels of nonlinearized constant-temperature anemometers were first passed through carefully matched 1 kHz cut-off low-pass filters then sampled at a frequency of 3 kHz (per channel) before being digitally recorded. The digital tape was subsequently processed on an English Electric KDF9 computer in the University of Sydney to yield as one of the first steps in the computation the required u and v signals as well as the product uv. The integral moments $\overline{u^n}$, $\overline{v^n}$ and $\overline{u^m v^n}$ were obtained directly from the digital records (of approximately 10 s duration) and not by forming the weighted integrals of the also-computed probability densities of u, v and uv. Despite the relatively short length of record used, the dispersion of the data for integral moments considered here was found to be small (less than 10 %). The nonlinearity of the anemometer was found to affect the skewness of u only for the points closest to the wall ($yU_\tau/\nu < 100$) but does not affect the skewness of v or the flatness factors of u and v. It therefore seems likely that the skewness of uv and, to a lesser extent, the flatness factor of uv may be slightly affected in the region close to the wall. Further details on flow conditions, surface geometry and data reduction may be obtained from Antonia & Luxton (1971*a*).

The measured skewnesses and flatness factors of $uv - \overline{uv}$ across the boundary layer are presented in figures 1 and 2 together with the predictions from (5) and (6), which make use of some of the measured moments of $\overline{u^n}$, $\overline{v^n}$ and $\overline{u^m v^n}$ up to the fourth order. The correlation coefficient r shown in figures 1 and 2 remains essentially constant over most of the extent of the layers, so that the assumption of a Gaussian joint probability density p_{uv} (i.e. retaining only terms involving r in relations (5) and (6)) would be essentially inadequate for predicting F and S. In the vicinity of the smooth wall, the measured flatness factor F of $uv - \overline{uv}$ (figure 1 (*a*)) increases as the wall is approached.† The F predicted from (6) follows the experimental trend quite closely but (6*a*) predicts only a small increase in F owing to the observed slight rise in the flatness factors of u and v in this region of the flow. For y/δ less than about 0·15 the skewness S predicted by (5) follows the experimental distribution (figure 1 (*b*)) closely but (5*a*) shows a noticeable departure. In the region of the layer corresponding to $0{\cdot}15 < y/\delta < 0{\cdot}30$, the characteristics of u and v are very nearly Gaussian and (6*a*) only slightly underestimates F whilst the S predicted from (5*a*) is essentially in accord with the experimental results and with the prediction of (5). In the intermittent region of the layer, relation (6) overestimates F, the departure from the experimental distribution becoming more marked with increasing y/δ. Equation (6*a*), on the other hand, significantly underestimates F. Analogous behaviour for the S predicted from (5) and (5*a*) is observed in figure 1 (*b*). In this outer region of the

† Recent measurements by Gupta & Kaplan (1972) show that F reaches a value at high as 100 well within the sublayer ($yU_\tau/\nu \simeq 4$, U_τ being the friction velocity). This result together with some instantaneous records of uv obtained by Willmarth & Lu (1972) as $yU_\tau/\nu = 30$ suggest that the uv signal is clearly intermittent in the viscous sublayer.

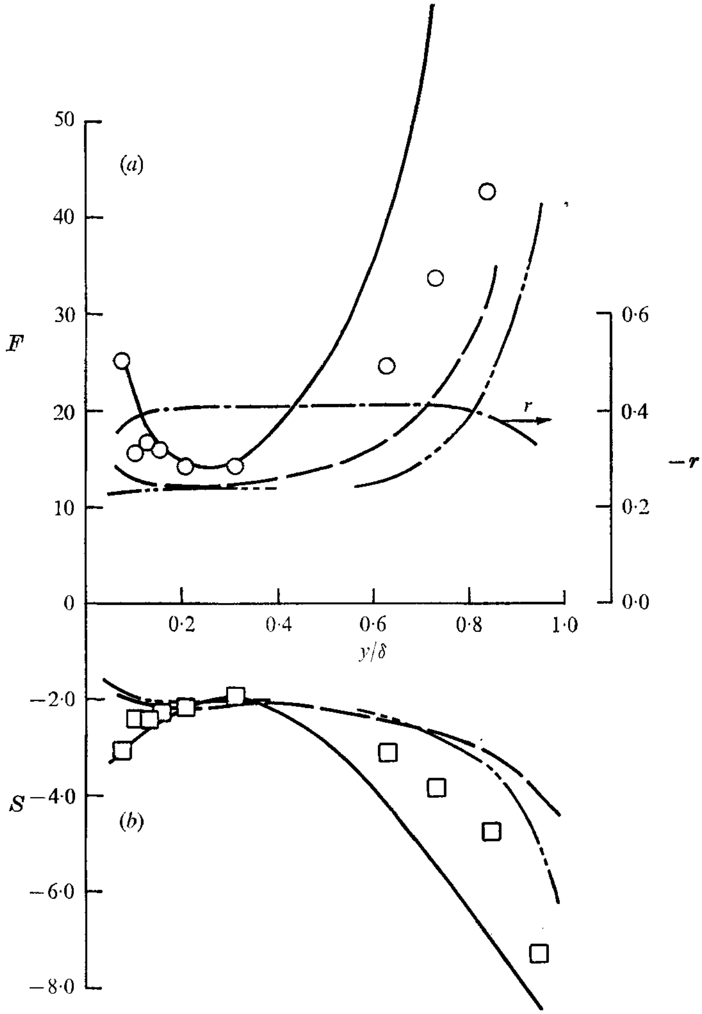

FIGURE 1. (*a*) Flatness factor and (*b*) skewness of *uv* in smooth-wall boundary layer. — - - —, prediction of model described in §5 using data of Kovasznay *et al.* (1970). (*a*) ○, experiment; ——, equation (6); – – –, equation (6*a*); —·—, experimental *r*. (*b*) □, experiment; ——, equation (5); – – –, equation (5*a*).

layer, the characteristics of u and v depart quite significantly from the Gaussian ones, the flatness factors of u and v reaching values close to 10 for y/δ near 1·0. It is unlikely that the fourth-order model leading to (5) and (6) is suitable for describing the characteristics of uv in this part of the flow.

In contrast with the smooth-wall results, the rough-wall distributions of F and S show a respective decrease and increase with proximity to the surface. Equations (5), (5a), (6) and (6a) are essentially in agreement with the experimental results. In the outer part of the layer, (6a) again underestimates F while (5a) overestimates S. Surprisingly, the predictions from (5) and (6) represent a reasonable approximation to S and F respectively in the outer region of the rough-wall layer. Little trust can be placed on this agreement however as the

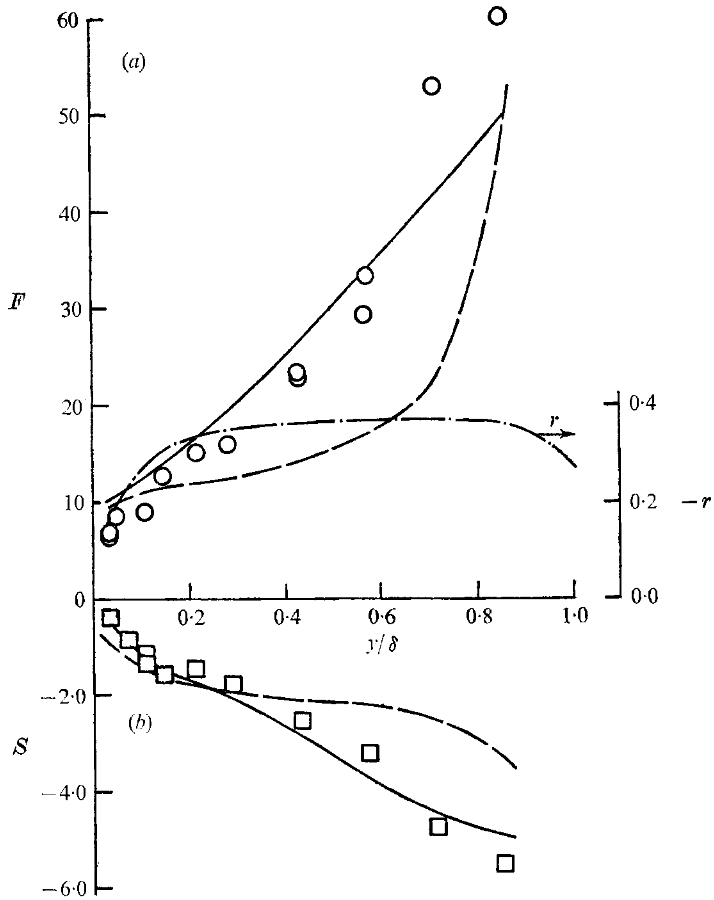

FIGURE 2. (a) Flatness factor and (b) skewness of uv in rough-wall boundary layer. (a) ○, experiment; ——, equation (6); – – –, equation (6a); —·—, experimental r. (b) □, experiment; ——, equation (5); – – –, equation (5a).

deletion of the cross-correlation terms involving k_{22}, k_{13} and k_{31} produces significant variations in the predicted F (see figure 3) and also S, at least for y/δ greater than 0·4. In the inner region of the layer, the predictions are not sensitive to the inclusion of some of the cross-correlation terms. It seems clear that, for the outer region of the layer, higher order terms must be included in the analysis of § 2 before the fourth-order moment of the product uv can be predicted to within the accuracy of available experimental data†. An alternative approach for the predictions of S and F in the intermittent zone of the flow, and one that seems more justifiable physically, is given in § 5.

† It should be noted that even for the weakly non-Gaussian turbulence obtained downstream of a grid, a sixth-order model for the joint probability density of the streamwise velocity fluctuations at two points separated in time is required for close agreement with the experimental time hyper-flatness factor (Frenkiel & Klebanoff 1967; Van Atta & Chen 1968).

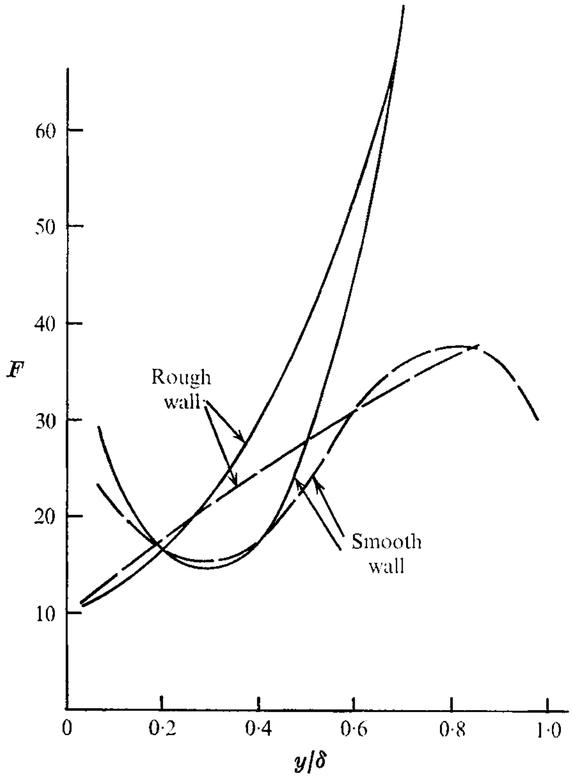

FIGURE 3. Effect of k_{22}, k_{13} and k_{31} on the flatness factor of uv. ——, equation (6) with $k_{22} = 0$; – –, equation (6) with $k_{13} = k_{31} = 0$.

4. Probability density of uv

The probability distribution P_w of the product $w = uv$ is given by

$$P_w(w) = \int_0^\infty du \int_{-\infty}^{w/u} dv\, p_{uv}(u,v) + \int_{-\infty}^0 du \int_{w/u}^\infty dv\, p_{uv}(u,v).$$

Differentiating with respect to w yields the probability density p_w:

$$p_w(w) = \int_0^\infty \frac{du}{u}\left[p_{uv}\left(u, \frac{w}{u}\right) + p_{uv}\left(-u, -\frac{w}{u}\right)\right]. \tag{7}$$

However, according to equation (2) for normalized u and v,

$$M_{uv}(\xi,\eta) = \exp\left[-\tfrac{1}{2}(\xi^2 + 2r\xi\eta + \eta^2) + \sum_{j+k>2} \frac{i^{j+k}}{j!\,k!} k_{jk}\,\xi^j\eta^k\right].$$

Equation (7) can be evaluated if M_{uv} is expanded in either of two ways:

(i) $M_{uv}(\xi,\eta) = \exp\left[-\tfrac{1}{2}(\xi^2+\eta^2)\right] \sum\limits_{j,k=0}^{\infty} C_{jk}\, i^{j+k}\xi^j\eta^k;$

(ii) $M_{uv}(\xi,\eta) = \exp\left[-\tfrac{1}{2}(\xi^2+2r\xi\eta+\eta^2)\right] \sum\limits_{j,k=0}^{\infty} D_{jk}\, i^{j+k}\xi^j\eta^k.$

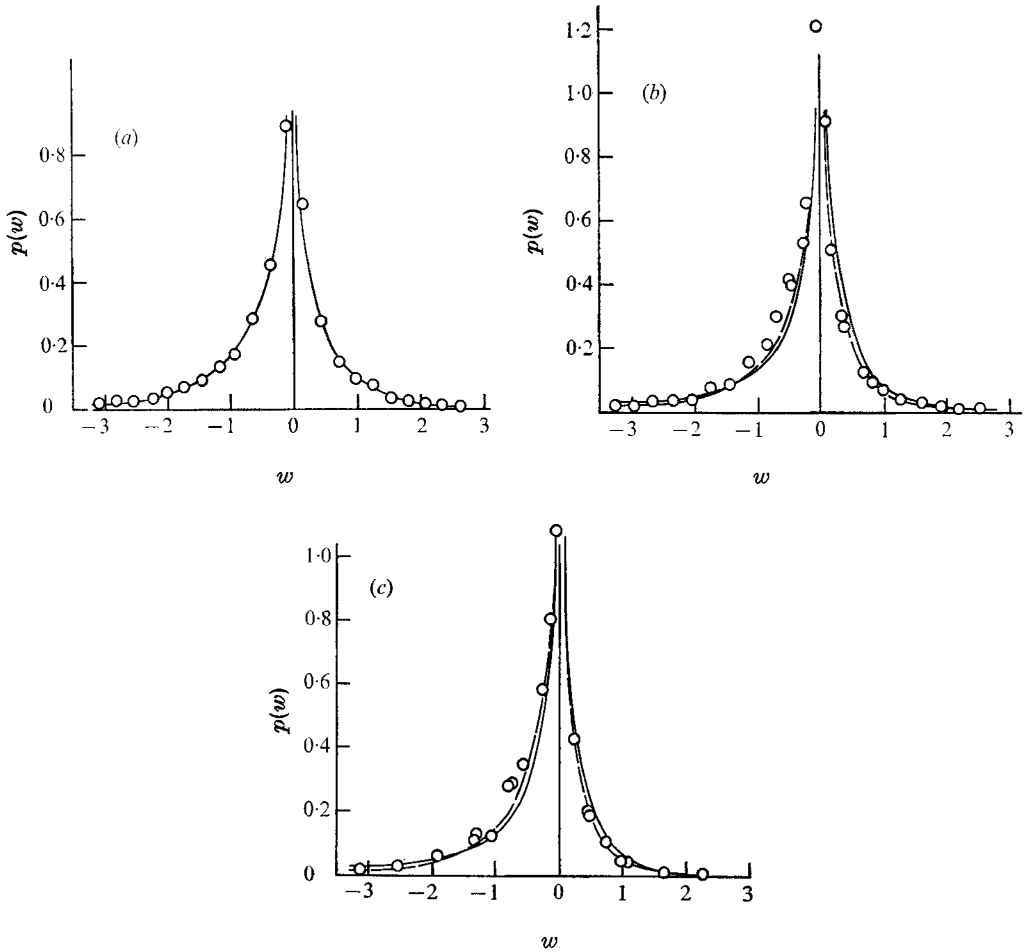

FIGURE 4. Probability density of uv. ○, experiment; ——, equation (11); – –, equation (12). (a) Rough wall, $y/\delta = 0{\cdot}071$. (b) Rough wall $y/\delta = 0{\cdot}57$. (c) Smooth wall, $y/\delta = 0{\cdot}632$.

Here C_{jk} is the coefficient of $x^j y^k$ in the power-series expansion of

$$\exp\left[rxy + \Sigma \frac{k_{jk}}{j!\,k!} x^j y^k\right],$$

so that

$$C_{00} = 1, \quad C_{10} = C_{20} = 0, \quad C_{11} = r, \quad C_{30} = \tfrac{1}{6}k_{30}, \quad C_{21} = \tfrac{1}{2}k_{21},$$

$$C_{40} = \tfrac{1}{24}k_{40}, \quad C_{31} = \tfrac{1}{6}k_{31}, \quad C_{22} = \tfrac{1}{4}k_{22} + \tfrac{1}{2}r^2,$$

together with the corresponding expressions with j and k interchanged. Similarly,

$$D_{00} = 1, \quad D_{jk} = 0 \quad \text{for} \quad j+k = 1, 2, \quad D_{jk} = k_{jk}/j!\,k! \quad \text{for} \quad j+k = 3, 4, 5.$$

The probability densities corresponding to (i) and (ii) can be found by doing the Fourier inversion term by term. Expression (i) yields the Gram–Charlier distribution

$$p_{uv}(u, v) = \frac{1}{2\pi} \sum_{j+k} C_{jk} He_j(u)\, He_k(v) \exp\left(-\tfrac{1}{2}u^2 - \tfrac{1}{2}v^2\right), \tag{8}$$

where the $He_j(u)$ are Hermite polynomials. Expression (ii) yields the generalized Gram–Charlier distribution

$$p_{uv}(u,v) = \frac{1}{2\pi(1-r^2)^{\frac{1}{2}}}\sum_{j,k}(-1)^{j+k}D_{jk}\frac{\partial^{j+k}}{\partial u^j\,\partial v^k}\exp\left[-\frac{u^2-2ruv+v^2}{2(1-r^2)}\right]. \tag{9}$$

Substituting (8) into (7) and using the symmetry of $He_j(u)$ (even for even j, odd for odd j) leads to

$$p_w(w) = \sum_{j+k\text{ even}}\frac{1}{\pi}C_{jk}\int_0^\infty He_j(u)\,He_k\left(\frac{w}{u}\right)\exp\left[-\frac{1}{2}\left(u^2+\frac{w^2}{u^2}\right)\right]\frac{du}{u}, \tag{10}$$

which is an infinite series of terms of the form

$$I_{lm} = \int_0^\infty u^l\left(\frac{w}{u}\right)^m\exp\left[-\frac{1}{2}\left(u^2+\frac{w^2}{u^2}\right)\right]\frac{du}{u}.$$

Using relation (4.5.29) from p. 146 of Erdélyi (1954) it may be shown that

$$I_{lm} = w^m|w|^{\frac{1}{2}(l-m)}K_{\frac{1}{2}(l-m)}(|w|),$$

where K is the modified Bessel function of the second kind. Substitution of this result into (10) and making use of the Bessel function recurrence relations leads, after some manipulation, to

$$\begin{aligned} p_w(w) = {}& \pi^{-1}K_0(|w|)\{(1+C_{22}+3C_{40}+3C_{04})+w(C_{11}-3C_{31}-3C_{13}) \\ & +w^2(C_{40}+C_{04}+C_{22})\}+\pi^{-1}|w|\,K_1(|w|)\{-2(C_{22}+2C_{40}+2C_{04})+w(C_{31}+C_{13})\}, \end{aligned} \tag{11}$$

where C_{jk} terms of order only up to four have been included. The corresponding result using the generalized Gram–Charlier distribution (9) is

$$\begin{aligned} p_w(w) = {}& \frac{\exp[rw/(1-r^2)]}{\pi(1-r^2)^{\frac{1}{2}}}\left\{K_0\left(\frac{|w|}{1-r^2}\right)\left[1+\frac{1}{(1-r^2)^2}\{3(D_{40}+D_{04})-3r(D_{31}+D_{13})\right.\right. \\ & +(1+2r^2)D_{22}\}+\frac{rw}{(1-r^2)^3}\{12(D_{40}+D_{04})-3r^{-1}(1+3r^2) \\ & \times(D_{31}+D_{13})+4(2+r^2)D_{22}\}+\frac{w^2}{(1-r^2)^4}\{(1+6r^2+r^4)(D_{40}+D_{04}+D_{22}) \\ & \left.-4r(1+r^2)(D_{31}+D_{13})\}\right]-\frac{|w|}{1-r^2}K_1\left(\frac{|w|}{1-r^2}\right)\left[\frac{1}{(1-r^2)^2}\{2(2+3r^2-3r^4)\right. \\ & \times(D_{40}+D_{04})-r(7+r^2)(D_{31}+D_{13})+2(1+4r^2)D_{22}\}+\frac{rw}{(1-r^2)^3} \\ & \left.\left.\times\{4(1+r^2)D(_{40}+D_{04}+D_{22})-r^{-1}(1+6r^2+r^4)(D_{31}+D_{13})\}\right]\right\}. \end{aligned} \tag{12}$$

When all the D_{ij} are set equal to zero the above expression reduces to the form corresponding to the assumption of a Gaussian joint probability density p_{uv}.

Expression (11) is compared in figure 4 with a few of the computed probability densities. In the rough-wall layer at $y/\delta = 0{\cdot}071$ (figure 4(*a*)) relation (11) is in good agreement with the experimental points. The result of (12) is virtually identical with that of (11) and has not been shown in figure 4(*a*). At $y/\delta = 0{\cdot}57$ on the rough wall (figure 4(*b*)) and at $y/\delta = 0{\cdot}62$ on the smooth wall (figure 4(*c*)) the predicted frequency of occurrence from (11) of moderately small negative values of w is appreciably smaller than the experimental distribution, but for the larger negative values of w expression (11) lies slightly above the experimental curve. Not unexpectedly, since its rate of convergence is faster, equation (12) represents a slightly better prediction for the experimental curves of figures 4 (*b*) and (*c*).

5. Properties of uv assuming intermittency

An alternative approach for the predictions of S and F in the intermittent zone of the flow is to assume that the probability densities of u and v are made up of the sums of the densities of these variables in the turbulent and irrotational parts of the flow, which is effectively an assumption of independence for the occurrence of these two states. Conditionally sampled measurements presented in Antonia (1972) indicate that the probability densities of u and v in both the turbulent and non-turbulent parts of the flow are close to being Gaussian. With less justification, we shall also assume that these two parts of the flow form stationary processes, so that their probability densities are independent of time, the instantaneous distance to the turbulent–non-turbulent interface, and so on. Because of the lack of experimental data, some such assumptions must be made. Data assumed known are the intermittency factor γ (the fraction of time for which the flow is turbulent) and the means and fluctuation intensities of u and v in both turbulent and non-turbulent zones of the flow.

The joint probability density of u and v is given by

$$p_{uv}(u,v) = \gamma p^T(u,v) + (1-\gamma)\, p^N(u,v),$$

where p^T and p^N are Gaussian distributions and the superscripts T and N denote turbulent and non-turbulent regions respectively. Multiplying by $u^j v^k$ and integrating gives

$$m_{jk} = \overline{u^j v^k} = \gamma m^T_{jk} + (1-\gamma)\, m^N_{jk}. \tag{13}$$

In the case where u and v have zero mean

$$\gamma m^T_{10} + (1-\gamma)\, m^N_{10} = \gamma m^T_{01} + (1-\gamma)\, m^N_{01} = 0,$$

whence

$$m^T_{10} = (1-\gamma)\,\mu_u, \quad m^N_{10} = -\gamma\mu_u, \quad m^T_{01} = (1-\gamma)\,\mu_v, \quad m^N_{01} = -\gamma\mu_v,$$

where $\mu_u = m^T_{10} - m^N_{10}$ and $\mu_v = m^T_{01} - m^N_{01}$, i.e. μ represents the difference between turbulent and non-turbulent means. In a turbulent boundary layer the conditionally sampled measurements of Kovasznay, Kibens & Blackwelder (1970) show that μ_u and μ_v reach maximum values of $-5\,\%$ and $2{\cdot}5\,\%$ respectively of the free-stream velocity. If σ^T_u, σ^T_v and r^T and σ^N_u, σ^N_v and r^N represent the standard deviations and correlation coefficients of u and v relative to the appropriate means in the T and N states respectively, we have

$$m^T_{20} = \sigma^{T2}_u + (1-\gamma)^2\mu^2_u, \quad m^T_{02} = \sigma^{T2}_v + (1-\gamma)^2\mu^2_v,$$

$$m^T_{11} = r^T\sigma^T_u\sigma^T_v + (1-\gamma)^2\mu_u\mu_v,$$

$$m^N_{20} = \sigma^{N2}_u + \gamma^2\mu^2_u, \quad m^N_{02} = \sigma^{N2}_v + \gamma^2\mu^2_v, \quad m^N_{11} = r^N\sigma^N_u\sigma^N_v + \gamma^2\mu_u\mu_v.$$

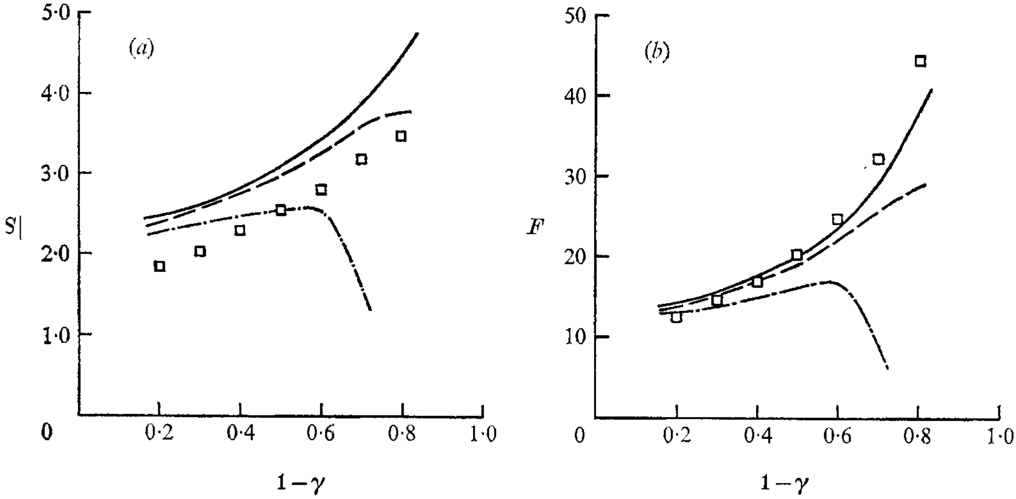

FIGURE 5. (a) Skewness and (b) flatness factor of uv in intermittent region of a shear flow. □, mixing-layer data (Wygnanski & Fiedler 1970). Boundary-layer data (Kovasznay *et al.* 1970; Blackwelder 1970): ——, $k_v/k_u = 0{\cdot}8$; – – –, $k_v/k_u = 1{\cdot}0$; — — —, $k_v/k_u = 1{\cdot}4$.

Since p^T and p^N are Gaussian, all their moments of order three and higher depend on those of orders one and two. These relations can be obtained by repeated integration by parts or by using cumulants. In particular, from (3),

$$\left.\begin{aligned} m_{22}^T &= m_{20}^T m_{02}^T + 2m_{11}^{T2} - 2m_{10}^{T2} m_{01}^{T2}, \\ m_{33}^T &= 3m_{11}^T(3m_{20}^T m_{02}^T + 2m_{11}^{T2}) - 6m_{10}^T m_{01}^T \\ &\quad \times (m_{20}^T m_{01}^{T2} + 3m_{11}^T m_{10}^T m_{01}^T + m_{02}^T m_{10}^{T2}) + 16m_{10}^T m_{01}^{T3}, \\ m_{44}^T &= 3(3m_{20}^{T2} m_{02}^{T2} + 24m_{20}^T m_{11}^{T2} m_{02}^T + 8m_{11}^{T3}) - 6(m_{20}^{T2} m_{01}^{T4} + m_{02}^{T2} m_{10}^{T4}) \\ &\quad - 96m_{11}^T m_{10}^T m_{01}^N(m_{20}^T m_{01}^{T2} + m_{02}^T m_{01}^{T2}) - 72m_{10}^{T2} m_{01}^{T2}(m_{20}^T m_{01}^T + 2m_{11}^{T2}) \\ &\quad + 32m_{10}^{T2} m_{01}^{T2}(3m_{20}^T m_{01}^{T2} + 8m_{11}^T m_{10}^T m_{01}^T + 3m_{02}^T m_{10}^{T2}) - 132m_{10}^{T4} m_{01}^{T4}, \end{aligned}\right\} \quad (14)$$

together with the same equations with superscript N. The first four cumulants of uv may be found using

$$\left.\begin{aligned} k_1 = m_{11}, \quad k_2 = m_{22} - m_{11}^2, \quad k_3 = m_{33} - 3m_{22}m_{11} + 2m_{11}^3, \\ k_4 = m_{44} - 3m_{22}^2 - 4m_{33}m_{11} + 12m_{22}m_{11}^2 - 6m_{11}^4. \end{aligned}\right\}$$

The standard deviation, skewness and flatness factor of uv are then given by

$$\sigma_{uv} = k_2^{\frac{1}{2}}, \quad S_{uv} = k_3/\sigma_{uv}^3, \quad F_{uv} = k_4/\sigma_{uv}^4 + 3.$$

Wygnanski & Fiedler (1970) used the conditional sampling technique in the mixing layer of a two-dimensional jet to obtain the turbulent and irrotational averages of u, v and uv, and of the intensities of u and v. The experimental values of γ, μ_u, μ_v, σ_u^T, σ_v^T, r^T, σ_u^N, σ_v^N and r^N in the high-speed side of the mixing layer have been used in the relations (1), (2) and (3) to obtain the skewness and flatness factors of uv shown in figures 5(a) and (b).

Corresponding conditionally sampled measurements in a zero-pressure-gradient turbulent boundary layer are available in Kovasznay *et al.* (1970) and

Blackwelder (1970). Unfortunately, σ_v^T and σ_v^N are not presented in these references. An attempt to estimate σ_v^N (and hence σ_v^T as m_{02} is known) was made by assuming that

$$\frac{m_{20}^N}{U_1^2} = k_u\left(\frac{y-y_0}{\delta}\right)^{-4}, \quad \frac{m_{02}^N}{U_1^2} = k_v\left(\frac{y-y_0}{\delta}\right)^{-4},$$

where k_u and k_v are constants, y_0 is the apparent origin of the fluctuations and U_1 and δ represent velocity and length scales respectively of the large energy-containing scale of the motion. The form of the above expressions was first predicted by Phillips (1955), who showed it to be asymptotically correct at large values of y/δ. A rather large amount of experimental evidence has however verified the existence of this form at quite small values of y/δ but the value of y_0/δ is ill-defined (Bradshaw 1967), whilst the constants k_u and k_v have been found to vary from flow to flow and appear to depend on experimental conditions for any given flow. Bradbury (1965) finds an average value for k_v/k_u in a two-dimensional jet in a slowly moving free stream of about 2·5, Bradshaw (1967) obtains a value close to 1·0 for a strongly retarded boundary layer whilst the mixing-layer results of Wygnanski & Fiedler (1970) indicate a value as high as 3·8. The results of figure 5 show that a value for this ratio close to or slightly smaller than 1·0 will yield a distribution of F in reasonable agreement with the distribution derived from the data of Wygnanski & Fiedler (1970). A slightly higher and probably more plausible value of k_v/k_u (Phillips (1955) predicts that $\overline{v^2} = \overline{u^2}+\overline{w^2}$) leads to an implausible decrease in F and $|S|$ towards the edge of the layer.

The resulting predictions for F and S using the data of Kovasznay *et al.* (1970) with $k_v/k_u = 0{\cdot}8$ are shown in figures 1(*a*) and (*b*) for comparison with the predictions of (2). For $y/\delta > 0{\cdot}65$, the predictions of the intermittent model qualitatively follow the experimental distributions but clearly underestimate F and $|S|$, whereas the predictions of the fourth-order non-intermittent model presented in § 2 had clearly overestimated F and $|S|$. For $y/\delta < 0{\cdot}4$ (γ has a value of 1 near $y/\delta = 0{\cdot}4$), the predictions of the intermittent model should agree with the values of F and S given by relations (5*a*) and (6*a*) for $k_{30} = k_{03} = k_{40} = k_{04} = 0$. These latter values are also shown in figure 1. The poor quantitative agreement between the intermittent-model predictions and the experimental data in the outer layer must be partly attributed to the non-Gaussianity of the velocity fluctuations in both the turbulent and non-turbulent parts of the flow and also to the uncertainty in the conditional data caused by the somewhat subjective formation of the intermittency function (see for example Kovasznay *et al.* 1970). The inclusion of the higher order (non-Gaussian) terms in the intermittent model should be straightforward but before this is attempted reliable conditionally sampled measurements are required.

6. Conclusions

The expressions for the skewness and flatness factor of uv derived by discarding cumulants of order greater than four are in good agreement with the experimental results in the inner regions of smooth- and rough-wall boundary layers. In the outer intermittent regions of the layers, relations (5) and (6) only qualitatively follow the experimental results. The predictions of S and F obtained for the intermittent regions by assuming Gaussian properties for the turbulent and irrotational fluctuations are not a significant improvement on the predictions of the fourth-order non-intermittent model. As the departures from Gaussianity of these fluctuations are not expected to be large, it is expected that a modified intermittent model should be adequate for predicting high-order moments of uv in the outer region of the boundary layer.

The work described in this paper represents part of a programme of research supported by the Australian Research Grants Committee, the Australian Institute of Nuclear Science and Engineering, and the Commonwealth Scientific and Industrial Research Organization.

REFERENCES

ANTONIA, R. A. 1972 *J. Fluid Mech.* **56**, 1.

ANTONIA, R. A. & LUXTON, R. E. 1971*a* *J. Fluid Mech.* **48**, 721.

ANTONIA, R. A. & LUXTON, R. E. 1971*b* *Dept. Mech. Engng, University of Sydney, Charles Kolling Res. Lab. Tech. Note*, no. F-31.

BLACKWELDER, R. F. 1970 Ph.D. dissertation, The Johns Hopkins University.

BRADBURY, L. J. S. 1965 *J. Fluid Mech.* **23**, 31.

BRADSHAW, P. 1967 *J. Fluid Mech.* **27**, 209.

ERDÉLYI, A. (ed.) 1954 *Tables of Integral Transforms*, vol. 1. McGraw-Hill.

FRENKIEL, F. N. & KLEBANOFF, P. S. 1967 *Phys. Fluids*, **10**, 507.

GUPTA, A. K. & KAPLAN, R. E. 1972 *Phys. Fluids*, **15**, 981.

KOVASZNAY, L. S. G., KIBENS, V. & BLACKWELDER, R. F. 1970 *J. Fluid Mech.* **41**, 283.

LIN, Y. K. 1967 *Probabilistic Theory of Structural Dynamics*. McGraw-Hill.

PHILLIPS, O. M. 1955 *Proc. Camb. Phil. Soc.* **51**, 220.

VAN ATTA, C. W. & CHEN, W. Y. 1968 *J. Fluid Mech.* **34**, 497.

VAN ATTA, C. W. & YEH, T. T. 1970 *J. Fluid Mech.* **41**, 169.

WILLMARTH, W. W. & LU, S. S. 1972 *AGARD Conf. Proc.* no. 93.

WYGNANSKI, I. & FIEDLER, H. E. 1970 *J. Fluid Mech.* **41**, 327.